


# Removing a single neuron in a vertebrate brain forever abolishes an essential behavior

Alexander Hecker<sup>a</sup>, Wolfram Schulze<sup>a</sup> , Jakob Oster<sup>a</sup>, David O. Richter<sup>a</sup>, and Stefan Schuster<sup>a,1</sup>

<sup>a</sup>Department of Animal Physiology, University of Bayreuth, 95440 Bayreuth, Germany

Edited by L. B. Vosshall, The Rockefeller University, New York, NY, and approved January 3, 2020 (received for review October 23, 2019)

The giant Mauthner (M) cell is the largest neuron known in the vertebrate brain. It has enabled major breakthroughs in neuroscience but its ultimate function remains surprisingly unclear: An actual survival value of M cell-mediated escapes has never been supported experimentally and ablating the cell repeatedly failed to eliminate all rapid escapes, suggesting that escapes can equally well be driven by smaller neurons. Here we applied techniques to simultaneously measure escape performance and the state of the giant M axon over an extended period following ablation of its soma. We discovered that the axon survives remarkably long and remains still fully capable of driving rapid escape behavior. By unilaterally removing one of the two M axons and comparing escapes in the same individual that could or could not recruit an M axon, we show that the giant M axon is essential for rapid escapes and that its loss means that rapid escapes are also lost forever. This allowed us to directly test the survival value of the M cell-mediated escapes and to show that the absence of this giant neuron directly affects survival in encounters with a natural predator. These findings not only offer a surprising solution to an old puzzle but demonstrate that even complex brains can trust vital functions to individual neurons. Our findings suggest that mechanisms must have evolved in parallel with the unique significance of these neurons to keep their axons alive and connected.

ablation phenotype | startle response | grandmother neuron | predator-prey | axon initial segment

The giant neurons found in the escape circuitry (1–5) and sensory centers (1, 6, 7) of many animals have always been instrumental in major breakthroughs in neuroscience—from the classic experiments in the squid axon to the discovery of axonal protein synthesis in the Mauthner (M) cell of teleost fish (8, 9). Despite their outstanding role in the study of proximate mechanisms, the ultimate reason for having and maintaining such gigantic neurons has received far less interest and poses major puzzles that have never been addressed. Specifically, in the M cell of teleost fish, experiments over the past decades have repeatedly shown that rapid escapes are still possible after removal of the giant M cell (8–20), suggesting that these starts could equally well be driven by smaller neurons, such as the smaller serial homologs MiD2cm and MiD3cm (8, 9, 12–14, 16, 20–22). Even the role of the rapid escapes for survival is not as clear as it seemed: The few studies available fail to detect a survival function of rapid escapes (23, 24), a survival value has been questioned on theoretical grounds (11–13, 25), and attempts to analyze the survival value of fast, short-latency responses show that responding quickly can even be a disadvantage: Survival depends, among many other aspects, on speed and maneuverability of the predator and its prey as well as the mechanism used for prey capture (26–28).

So, when the role of the M cell in escape behavior can be taken over by smaller neurons and when M cell-driven rapid escapes are not of clear survival function, what could then be the reasons for having the giant M cell? Is it a “leftover” that is tied to the basic plan of a fish? The M cell forms remarkably early, in the late gastrula (29), and its major function could be to guide neuronal growth. However, even then it would not be clear why such guidance could not be achieved by smaller versions of the M cells.

Here we present a series of experiments that were specifically aimed at solving the puzzle of what is the ultimate role of the M cell. Using larval and adult zebrafish, we discovered that ablation experiments require the utmost care to ensure that not only the soma but also the axon has degenerated. If one waits until the axon is lost, then the ability to escape rapidly is also lost completely. Furthermore, experiments with an ecologically relevant voracious predator of zebrafish larvae in the wild show that this loss translates directly into a loss of fitness. Moreover, loss of the cell could never be compensated throughout the lifetime of the fish. Our findings demonstrate a clear survival function of the giant M cell. They thus solve a major evolutionary puzzle and end the controversy of whether M cells are truly needed to initiate the fastest escapes. Furthermore, we show that an individual giant neuron in the vertebrate CNS can play a crucial role for survival—at the full risk that losing that neuron does affect survival.

## Results

**Simultaneously Monitoring Behavior and Decay of the Cell.** Most earlier ablation work controlled for the absence of the M cell soma but not for the absence of the axon (10–18, 20). Most importantly, it was previously unknown if and how long the axon would survive after the soma was gone. To examine these important issues, we used two-photon laser irradiation in transgenic zebrafish larvae. This allowed us to specifically irradiate the M cells and to induce Wallerian-like degeneration (30, 31) in either one or both M axons of a larva while demonstrably leaving associated structures intact (*SI Appendix*, Fig. S1 and *Movies S1* and

## Significance

The Mauthner cell is the largest neuron known in the vertebrate brain and, in fish, mediates rapid escape behavior. Ablating this neuron has repeatedly failed to eliminate rapid escapes, a survival role of these escapes has not been supported experimentally, and it is unknown which advantage the enormous size and complexity of the cell conveys. By taking care to ensure ablations remove not only the soma but also the giant axon, we find that rapid escapes are lost forever and that this loss directly affects survival in predator-prey assays. The Mauthner cell thus is an example in which a survival-critical function depends on an individual neuron whose axon appears to have unusual capacities to remain functional after severe injury.

Author contributions: A.H. and S.S. designed research; A.H., W.S., and J.O. performed research; A.H., W.S., and D.O.R. contributed new reagents/analytic tools; A.H., W.S., and S.S. analyzed data; and A.H. and S.S. wrote the paper.

The authors declare no competing interest.

This article is a PNAS Direct Submission.

This open access article is distributed under [Creative Commons Attribution-NonCommercial-NoDerivatives License 4.0 \(CC BY-NC-ND\)](https://creativecommons.org/licenses/by-nc-nd/4.0/).

<sup>1</sup>To whom correspondence may be addressed. Email: stefan.schuster@uni-bayreuth.de.

This article contains supporting information online at <https://www.pnas.org/lookup/suppl/doi:10.1073/pnas.1918578117/-DCSupplemental>.

First published January 30, 2020.

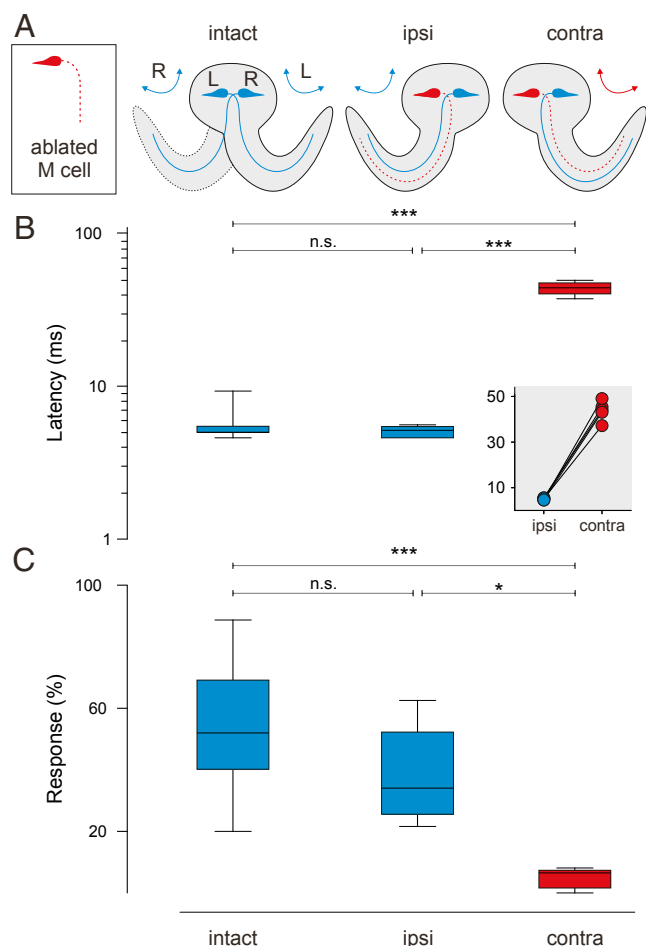


**Fig. 1.** The giant axon of the M neuron is essential for escape performance. (A) Outline of the idea to use unilateral ablations: An action potential in one of the two M cells elicits powerful contraction of the contralateral body side, causing it to bend (Left). After unilateral ablation of the soma and axon (red), only bending commanded by the ablated contralateral cell body should be affected, but bending to the other side should not. Unspecific side effects of ablation could thus be tested by comparing escapes made toward that side in the unilaterally ablated larvae with escapes made by untreated siblings L, left; R, right. (B and C) Escape latency (B) and release probability (C) in untreated control larvae ( $n = 862$  escapes from 18 larvae) and in ablated larvae for escapes that either could use the remaining cell (ipsi;  $n = 138$  escapes from 5 larvae) or not (contra;  $n = 43$  escapes from 5 larvae). Significance is as indicated (one-way ANOVA; latency: \*\*\* $P < 0.0001$  intact and ipsi vs. contra;  $P = 1$  intact vs. ipsi; probability: \*\*\* $P < 0.0001$  intact vs. contra; \* $P = 0.02$  ipsi vs. contra;  $P = 0.2$  intact vs. ipsi). n.s., not significant. (B, Inset) Side-specific increase in latency in each individual unilaterally ablated larva.

S2). Furthermore, we developed techniques that allowed us to monitor—in the same larva—both the state of its degenerating M axon and the larva's escape performance over the long time it took until the complete decay of the axon (SI Appendix, Fig. S1 and Movie S1). To probe escape performance at various degeneration stages of the axon, we selected a stimulus that demonstrably also activated the homologous neurons that are thought to compensate for the loss of the M cell (SI Appendix, Fig. S2) (8, 9, 14, 16, 20–22). Surprisingly, this approach revealed that a unilateral complete loss of one of the axons of the two M neurons specifically abolishes those rapid escapes (contralateral to where the soma of the missing M neuron was) that would have recruited the missing axon (9, 14) (Fig. 1A). Exploiting the symmetry of the system for an intrinsic control, we found that when the very same individual larva produced escapes that could

recruit the remaining intact M axon, these were not statistically different—both in response time (latency) and release probability—from escapes made by completely untreated siblings (latency:  $P = 1$  for intact vs. ipsilateral; Fig. 1B; one-way ANOVA;  $n = 862$  and 150 escapes from  $n = 18$  and 5 larvae; response probability:  $P = 0.2$  for intact vs. ipsilateral; Fig. 1C; one-way ANOVA;  $n = 1,572$  and 440 stimulations from  $n = 18$  and 5 larvae). This important control shows directly that the effect was not due to unspecific side effects of the ablation or of the general treatment. Our findings thus suggest that it may have been the absence of the particular individual axon that caused the massive drop in performance.

#### An Intact Axon Initial Segment Is Necessary for Rapid Escape Behavior.

We next discovered that two specific aspects of escape behavior, its threshold and its performance characteristics, were mediated by two different compartments of the M cell (Fig. 2A). When only the

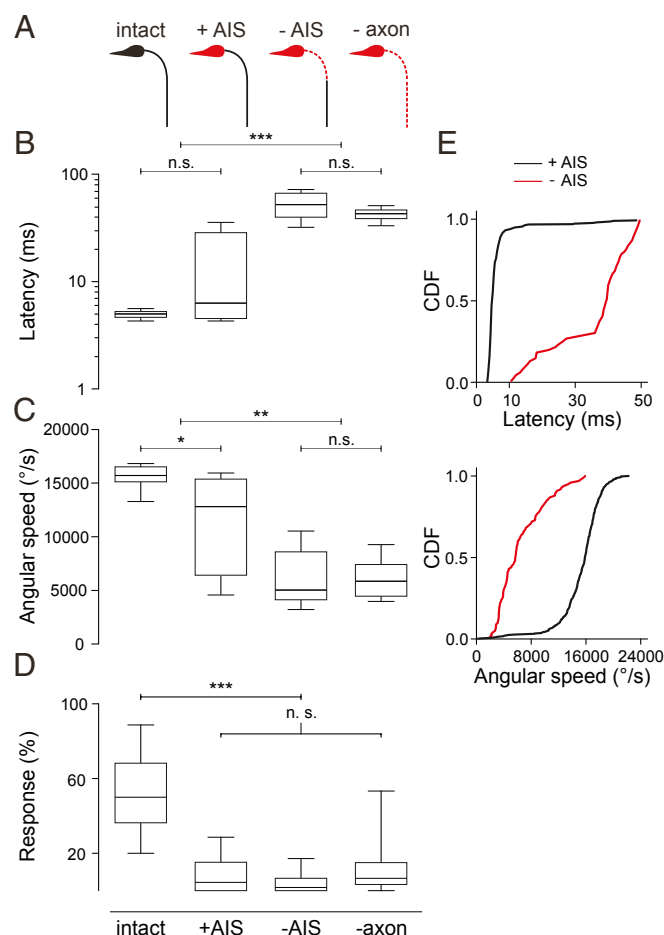


**Fig. 2.** All inputs that can rescue escape performance after loss of the M cell soma are sampled at the axon initial segment. (A) Stages of a degenerating M cell: still completely intact; soma absent but axon initial segment and axon intact (+AIS); without initial segment (–AIS) but remaining axon intact; also axon gone (–axon). (B–D) Latency (B), angular speed (C), and release probability (D) for escapes of larvae in which the escape would have recruited the (contralateral) cell in one of the stages shown in A. Boxplots are based on (from left to right)  $n = 258, 15, 22, 77$  escapes from  $n = 9, 4, 7, 13$  larvae for escape performance and  $n = 9, 6, 13, 15$  larvae for probability, respectively. (E) Cumulative distribution function (CDF) of latency (Top) and of average angular speed (Bottom) of escapes with (+AIS;  $n = 406$  escapes,  $n = 15$  larvae) and without axon initial segment (–AIS;  $n = 100$  escapes,  $n = 15$  larvae) to show how axon state predicted escape performance. \* $P < 0.05$ ; \*\* $P < 0.01$  and \*\*\* $P < 0.001$ , one-way ANOVA with Bonferroni-corrected  $t$  tests. n.s., not significant.

soma was absent but the axon was intact, the fish could still produce rapid escapes just as found in all earlier studies (8–20). However, when the soma and the initial segment of the axon (AIS) were lost, no rapid short-latency escapes occurred, regardless of whether the remaining axon was still present or not (Fig. 2B;  $n = 258, 15, 22, 77$  escapes from  $n = 9, 4, 7, 13$  larvae; one-way ANOVA with Bonferroni-corrected  $t$  tests:  $P$  values: intact vs. +AIS: 0.86; –AIS vs. –axon: 0.12). Additionally, the loss of the AIS also resulted in a massive decline in angular speed of the escape maneuvers and this effect was also independent of the presence of the remaining axon (Fig. 2C;  $P$  values: intact vs. +AIS: 0.04; +AIS vs. –AIS: 0.006; +AIS vs. –axon: 0.002). Removing the soma thus does not remove the capacity of the system to, in principle, produce rapid escapes. So, in a logical sense, not the soma but the AIS is necessary for the occurrence of rapid escapes. However, this does not mean that the soma and its huge dendrites were dispensable: Response probability was dramatically reduced when the soma was lost, regardless of whether the axon and the AIS remained intact or not (Fig. 2D; intact vs. other groups:  $P < 0.0001$ ;  $n = 9, 6, 13, 15$  larvae). Fig. 2E shows how the presence of the initial segment of the M axon (AIS) predicted the drastic changes in latency (upper) and in angular speed (lower) of the escapes. Absence of the AIS predicts a clear increase in latency—with a complete absence of short-latency escapes—and a massive drop in angular speed of the escape turns made. It is important to stress that the time after which the AIS had been lost varied dramatically across the individual larvae—at least by 20 h (SI Appendix, Fig. S1C). This implies that it was not the time after soma ablation (or after laser treatment) per se that predicted the massive drop in performance shown in Fig. 2E but the availability or absence of the AIS. Moreover, Fig. 2E also shows that as soon as the axon had degenerated beyond its axon initial segment, no high-speed, short-latency escapes were observed anymore. The starts that were still seen, at reduced probability, after the AIS was

gone (i.e., –AIS and –axon in Fig. 2D), were all, and in each individual, of substantially longer latency (SI Appendix, Table S1). In summary, the AIS of the M cell is required for high-speed, short-latency escapes, but the soma is required for efficiently releasing such starts.

#### A Direct Approach at the Ultimate Function of Having Giant Neurons.

So far, our findings have established that the loss of the axon of a single neuron drastically affects escape behavior. Since the function of the desomatized axon was previously unknown, our findings also explain why the effect so long defied discovery in one of the best studied neurons in the vertebrate brain (8, 9). The drastic effects of removing just one neuron are particularly unexpected for a crucial behavior such as escaping. It is therefore important to examine if compensation might be possible in other ways, for example by resorting to other behavioral strategies such as a “freezing response” or by increased alertness (32–34). Furthermore, the mix of sensory cues that emanates from a real predator could potentially stimulate additional circuits which might lead to far less dramatic effects than those we found using simple acoustic stimuli. Finally, it has been argued that even strong kinematic changes in the escapes would not affect survival (11–13, 25). So, we needed to examine directly if and to what degree the absence of the M cell would translate to a decrease in the chances of survival. We therefore developed an assay in which groups of zebrafish larvae with completely ablated M cells (including their axons) and various control zebrafish larvae faced damselfly nymphs, a major natural predator of zebrafish larvae in the wild (35, 36) (Movies S3 and S4). Assays were run in parallel in several tanks, each with a hungry nymph waiting (Fig. 3A–C). We analyzed the capability of the larvae to escape the strikes of their predator in either 1) experimental groups in which four bilaterally M axon-ablated larvae and four untreated *casper* larvae were placed in containers, each with a single

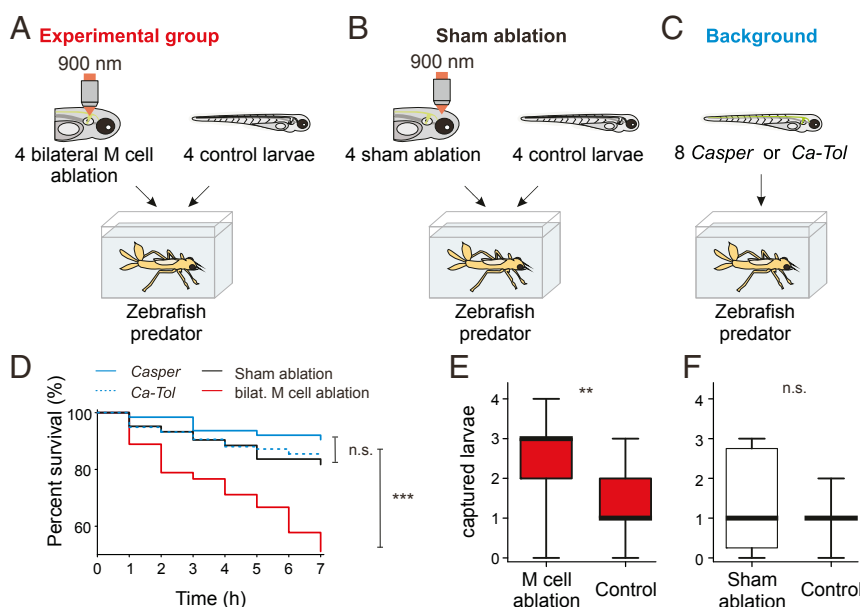


**Fig. 3.** Direct test of the survival value of having the giant M neuron. (A–C) After a preparation phase, individual last-instar damselfly nymphs (a predator of zebrafish larvae) were combined with eight zebrafish larvae. Ablated larvae had either both M axons (A) or two cerebellar neurons (B) ablated. (A) The experimental groups ( $n = 11$  groups) were mixed groups each of four M neuron-ablated larvae and four *casper* larvae. (B) Each procedural control group ( $n = 13$  groups) contained four sham-ablated larvae and four nonablated *casper* larvae. (C) Additional background control groups contained either eight untreated *Ca-Tol-056* larvae ( $n = 15$  groups) or eight *casper* larvae ( $n = 8$  groups). (D) Significant difference between capture rates in M cell-ablated larvae versus each of the three controls (\*\*\* $P < 0.0001$ , log-rank test) and no significant difference among all control, background, and sham-ablated fish ( $P > 0.12$ , log-rank test). (E and F) Analysis of the survivors at the end of the experiment (i.e., after 7 h) using their fluorescence signals confirms higher capture rates of M neuron-ablated fish (E; \*\*\* $P = 0.008$ , Mann–Whitney  $U$  test) but no higher capture rate of sham-ablated fish (F;  $P = 0.64$ , Mann–Whitney  $U$  test). Boxplots show capture rates as determined in the individual groups (medians are indicated by thick black horizontal lines).

nymph (Fig. 3A), 2) mixed groups of four sham-ablated (ablation of two cerebellar neurons) and four untreated *casper* larvae (Fig. 3B), or 3) homogeneous groups of eight untreated larvae of one of two zebrafish strains [Fig. 3C; *casper* or *Ca-Tol-056* (37, 38)]. We used the mixed groups to provide a comparative view of how affected individuals would fare if unaffected individuals were also available to the predator. When we counted the uncaptured larvae every hour it was immediately apparent that the groups that contained the M axon-ablated larvae had significantly fewer survivors than any of the three control groups (Fig. 3D; log-rank,  $P < 0.0001$ ). In contrast, no differences could be detected in survival between the control groups (log-rank,  $P > 0.12$ ; Fig. 3D, blue and black lines). To directly see which of the fish in the experimental (mixed) group were captured—either the M neuron-ablated or the control individuals—we checked all surviving fish at the end of the experimental session (i.e., after 7 h) under fluorescence illumination to tell the control and the ablated survivors apart (from the presence or absence of GFP expression; *Materials and Methods*). This analysis confirmed that the high capture rates in the experimental group (Fig. 3D, red) could indeed be attributed to the larvae with ablated M axons. Absence of the M axons significantly reduced the likelihood of escaping the predatory strikes of damselfly nymphs compared with the simultaneously present control larvae (Mann–Whitney  $U$  test,  $P = 0.008$ ; Fig. 3E; medians are indicated by heavy black lines). Furthermore, the effect cannot be attributed to the procedure as there is no difference between the sham-ablated and completely untreated larvae (Mann–Whitney  $U$  test,  $P = 0.64$ ; Fig. 3F). Hence, our discovery of a drop in kinematic performance after losing the M cell translates directly to a clear drop in the ability to survive the attacks of an ecologically relevant predator.

**Once the Cell Is Lost, a Behavioral Function Is Also Lost Forever.** We next examined whether the drastic consequences of losing an M axon early during ontogeny might be compensated during maturation of the larval nervous system or later during the months of life as an adult fish. To examine this possibility, we established procedures that allowed us to rear unilaterally ablated larvae together with their untreated siblings (Fig. 4A). This way, we could reexamine the early effects that the ablations had in the larvae and compare them with the effects found 5 mo later in the adults. Remarkably, the absence of a single M cell still caused the specific effects on response probability and on latency as it did—about half a year before—in the larva. Starts that could not recruit an M axon were far less likely than were starts shown by the same fish that could recruit the remaining M axon (Fig. 4B; Student's  $t$  test,  $P < 0.0001$ ;  $n = 1,880$  stimulations from 13 adults; cf. Fig. 1A). Furthermore, starts that would be commanded by the absent M cell had significantly increased escape latency and reduced angular speed (Fig. 4C–E; latency: Mann–Whitney  $U$  test,  $P < 0.0001$ ; angular speed: Student's  $t$  test,  $P < 0.01$ ;  $n = 515$  escapes from 13 adults) compared with the starts the same individual made when it could recruit the remaining axon. These important intrinsic controls thus show that the strong effects of the absence of one single M neuron remained uncompensated even during maturation of the larva and in the life as an adult fish.

## Discussion

The M cell is the largest neuron in the vertebrate brain. Nevertheless, it was a mystery why this large and presumably costly neuron is needed: Ablating the M cell repeatedly failed to cause a complete loss of the fastest M cell-mediated escapes (8–20), suggesting that loss of the cell can be compensated by using smaller neurons (8, 9, 12–14, 16, 20–22) or that the giant axon is needed for entirely different reasons, for example, for switching off competing motor programs (11–13, 25). Here we report two discoveries that 1) solve this puzzle in an unexpected way, 2)

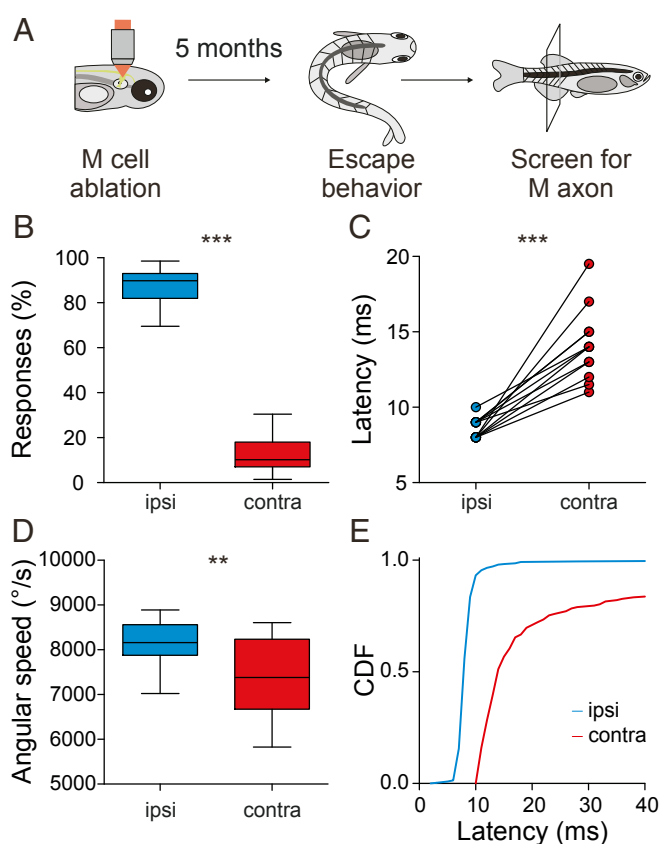


**Fig. 4.** Early loss of the M axon can never be compensated in later life. (A) Larvae with unilaterally ablated M axons (Fig. 1) grew up for 5 mo together with unablated siblings. After double-blind examination of their escape behavior, the fish were killed to check which, if any, M axon was missing. (B) As in the larvae, escapes were still predominantly to the side that could use the intact neuron (Student's  $t$  test,  $***P < 0.0001$ ;  $n = 1,880$  stimulations from 13 fish; see Fig. 1 for a definition of ipsi and contra). (C) Latency was also always significantly higher in those escapes, performed by the same individual zebrafish, that could not recruit an M cell (Mann–Whitney  $U$  test,  $***P < 0.0001$ ;  $n = 515$  escapes from 13 fish). Circles with connected lines show median latency in the same individual fish when an M cell could be recruited or not. (D) Mean angular speed in escapes that could not recruit an M cell was significantly lower (Student's  $t$  test,  $**P = 0.0089$ ;  $n = 515$  escapes from 13 fish). (E) Cumulative distribution function (CDF) of escape latency ( $<100$  ms) for escapes that either could ( $n = 353$  escapes) or could not ( $n = 162$  escapes) recruit the remaining M axon clearly shows a shift in minimum latency even in the adult fish.

allow directly addressing the ultimate role of the cell for survival, and 3) draw attention to several remarkable properties of the isolated giant M axon that suggest exciting new avenues for research. We show that the giant axon can survive ablations of its soma and remain functionally connected to sensory inputs and to its motor output circuitry for a surprisingly long time during which it is still capable of driving rapid escapes. We also show that all inputs that can recruit the axon after loss of the soma and dendrites are exclusively received in the axon initial segment so that the decisive role of the axon cannot be seen when ablations are not precisely restricted to the soma but also affect, for instance, the spiral fibers (*SI Appendix*, Fig. S1). We find no evidence in support of the presently accepted view that the so-called M series, composed of the M cell and its two serial homologs, or other neurons would compensate for the complete absence of the M cell (9–18, 20, 25): After the M axon is lost, dramatic changes in escape performance and in survival become readily apparent and are never fully compensated, not even later in life.



A survey of previous ablation work suggests that there were two major reasons why the dramatic effects of a complete removal of the M cell have defied discovery for such a long time. Either there were strong off-target effects of the ablation (19) or the ablation was incomplete at the time of behavioral monitoring. All papers that used laser ablation report that the remaining axon was intact when the behavioral experiments were done, so that it is likely that the axon initial segment was intact at least in some experiments. In some of these studies, behavioral testing has been carried out so early that (from our findings in *SI Appendix*, Fig. S1C) it cannot be ruled out that in some cases somata and dendrites were still intact (14, 17, 20). All earlier studies did still report short-latency escapes (in the sense of Fig. 2E) after ablation. One study reports a clear decline in escape probability (15); others explicitly state no effect on response probability (17, 19). In summary, our findings should draw attention to the level of care needed to interpret ablation phenotypes: Surviving compartments can still remain functional, and evidence for the absence and death of all compartments is needed. A parallel case is provided in the starburst amacrine cell, a key player in retinal processing of movement direction. Here, laser ablation work had suggested that direction selectivity did not require starburst amacrine cells (39). However, when a genetic approach was later used that demonstrably completely removed these cells, directional processing was compromised (40). This suggests that after laser ablation, compartments of the starburst amacrine cells also still have contributed to functionality at the time of experimental testing. Great care is also needed when inferring the relevance of AIS input relative to dendritic/somatic input after soma ablations: It is likely that the huge soma acts as a current sink for AIS inputs, so that ablating the soma would, after the membrane has healed, remove this sink, which would automatically increase the efficiency of the AIS inputs. This would be exactly what is needed to quickly up-regulate the remaining input into the surviving M axon. However, it clearly would not mean that these inputs are equally efficient when the large soma and dendrites of the cell are still present. In fact, our data directly show a massive drop in response probability that remained uncompensated from the early larva to the adult fish (Fig. 4B).

Our findings allow simple and direct experiments to determine the ultimate function of the starts driven by the giant M cells. Such experiments were missing, although their importance has repeatedly been emphasized (11–13, 25, 28). For instance, it has been argued that even an about 4-ms decrease in average latency would displace the fish only by a few insignificant millimeters from its initial position (11, 13). Without actual experiments, it is also unclear whether the animal could switch to other equally successful behavioral strategies and what would be the actual importance of short-latency starts (12, 13, 23–28). By completely removing the cells (including the giant axon), we could directly probe how the absence of M cell-driven rapid escapes affect survival in encounters with an ecologically relevant, voracious predator (35, 36). We find that for escaping the targeted ballistic strikes of damselfly nymphs, having an M cell clearly is of advantage. Our findings would also allow experiments that could help to decide for what types of predators M cell-driven starts are helpful. For instance, short-latency escapes may indeed be of little help in encounters with suction feeders (23, 24). The notion that the giant axon-mediated escapes would not actually be of survival value (10–13, 25), however, can clearly be dismissed.

Our findings have several far-reaching consequences and open up exciting new avenues: First, we demonstrate that the axon initial segment is the only site where inputs [such as from the spiral fiber neurons (17, 41–44)] can be fed into the remaining axon once the soma is lost. This means that all relevant inputs into the intact cell (i.e., dendritic, somatic, and via the AIS) can be detected by intracellularly recording in the soma. Among the

many prospects this entails is the use of the M neuron as a bottleneck for checking and calibrating brain-wide activity maps (45, 46). For instance, a guided iterative way to improve the accuracy and completeness of map data would be to detect failures in predicting simultaneous recordings made from the bottleneck neuron (during a behavior mediated by it). This should be an invaluable guide to eventually arrive at the temporal and spatial resolution needed for the ultimate goal of connectomics: relating brain-wide activity to behavior.

Second, since the individual M neurons are true bottlenecks, our findings suggest that powerful mechanisms should exist to ensure the survival of the M axon and its maintained functional connectivity with input and output pathways. Despite fascinating earlier reports—also in other giant axons (47–49)—it is not known which aspects that entails in detail, how mechanisms for survival of giant axons are distributed across the various giant neurons found in the animal kingdom, and what could be the mechanistic basis for their survival. The size and outstanding accessibility (8, 9) of these axons make them ideal candidates for in-depth analysis of the underlying mechanisms. Our findings illustrate that high pressures exist to evolve mechanisms to keep the axon alive and its connections to inputs and outputs fully functional. It is not hard to see that the evolutionary constraints predict the discovery of remarkable and potentially important mechanisms.

Third, our findings do not support the generally accepted view that sophisticated brains never trust vital behaviors to individual neurons and that uniquely important neurons such as the infamous mother or grandmother cells cannot exist in the vertebrate brain (50, 51). At least the giant M neuron does play a unique role: Its absence means the loss of a function with a measurable survival value. This suggests that high evolutionary pressures have existed for mechanisms that maintain the integrity and functionality of the precious axons of the M cell at all costs—even after severe injuries.

## Materials and Methods

**Zebrafish.** Zebrafish (*Danio rerio*) were kept in our fish housing system at 28.5 °C. Embryos were raised at 28.5 °C on a 12-h:12-h light/dark cycle in E3 medium (5 mM NaCl, 0.17 mM KCl, 0.33 mM CaCl<sub>2</sub>, 0.33 mM MgSO<sub>4</sub>·7H<sub>2</sub>O, 10<sup>−5</sup>% methylene blue in dH<sub>2</sub>O). All experiments were approved according to the German law on animal welfare. Behavioral studies were started at 5 dpf (days post fertilization). Larvae (*Ca-Tol-056*) were generated by crossing *Tol-056* (38) with pigmentless *casper* [*mitfa*<sup>w2/w2</sup>; *mpv17*<sup>g9/a9</sup>] (37). Ablations were performed at 5 dpf, except for the ablations in the predator–prey tests (4 dpf). Experiments on adults involved zebrafish with uni- or bilateral M cell lesions at 5 dpf that were raised together with unablated siblings for 5 mo. To confirm distributed activity in response to our stimulus, we retrogradely injected Oregon green 488 BAPTA-1 dextran into 5-dpf larvae of the *casper* strain. Subsequent imaging was then performed at 6 dpf. Specificity of the ablations was confirmed in 5-dpf larvae of the *Ca-Tol-056* strain.

**Damselfly Nymphs.** Damselfly nymphs (*Coenagrion puella*; last instar) were collected from external concrete basins at the University of Bayreuth with naturally occurring nymphs. During a preparation phase, nymphs were kept individually in plastic boxes at 18 °C with fresh water and waterweed (*Elo-dea* sp.) and each fed three chironomid larvae on the first and the fifth day after capture. This phase was intended to ensure a comparable state of hunger across the nymphs. After the experiments, nymphs were transferred back to the basins.

**Ablation of M Cells.** *Ca-Tol-056* larvae were anesthetized in 0.04% MS-222 and embedded in 1.5% low-melting-point agarose (Sigma-Aldrich) with their dorsal side up in a small Petri dish. An 80-MHz titanium:sapphire multiphoton excitation laser (pulse width <100 fs; Mai Tai DeepSee; Spectra-Physics) tuned to 900 nm in a two-photon laser-scanning microscope (Leica TCS SP5 II with HCX IRAPO L, 25.0 × 0.95 water immersion objective; Leica Microsystems) was used to ablate the M cells. Prior to ablation, a z stack (100 images, each 295 × 295 μm) of the two M cells (somata and axons) was taken for later comparison using low laser energy. For ablation, sufficiently high laser energy was focused onto the M cell soma in a region that contained

the nucleus. Exposure time was 136 s (100 scan repeats of the adjusted focal plane with a scan speed of 400 Hz and a resolution of 512 × 512 pixel; 9.23 × 9.23 μm). Larvae were then allowed to swim freely but were briefly (in less than 20 min) embedded, imaged, and subsequently freed again at set times after laser treatment (after 6, 20, and 44 h) to check the state of the M cell soma and axon. To create [Movie S1](#), we ablated the M cell unilaterally and imaged z stacks (100 images; 512 × 512 pixel; 590 × 590 μm) every 5 min for a total of 44 h.

**Immunohistochemistry.** *Ca-Tol-056* larvae (5 dpf) were fixed in 2% 1-ethyl-3-(3-dimethylaminopropyl) carbodiimide-hydrochloride or 2% paraformaldehyde (PFA) in ddH<sub>2</sub>O for 3 h at room temperature. Larvae were washed six times in PBSTx (1% Triton X-100 in phosphate-buffered saline [PBS], wt/vol) in 1.5-mL Eppendorf tubes with stainless steel mesh bottoms. Specimens were then blocked for 1 h in 5% NGS (normal goat serum) in PBSTx. Primary and secondary antibodies were diluted in 5% NGS in PBSTx at 22 °C for 48 h. Mouse anti-neurofilament-associated protein (1:40; DSHB; 3A10), rabbit anti-GFP (1:1,000; Thermo Fisher Scientific), or mouse anti-Cx35/36 (1:200; Millipore) was used as primary antibody. Goat anti-mouse Alexa Fluor 555 (1:500; Thermo Fisher Scientific) and goat anti-rabbit Fab2 Alexa Fluor 488 (Cell Signaling Technology) were used as secondary antibodies. Stained larvae were washed and then cleared in glycerol/PBS: 30/70 for 30 min, 50/50 for 1 h, and glycerol/PBS 70/30 overnight. The larval brains were dissected out and mounted on coverslips in Mowiol. Cx35/36 staining was examined using an Olympus Fluoview FV1000 confocal microscope with UPLSAP060XS objective. The larval brains were optically sectioned (106 × 106 × 250 μm; 4-μm pixel dwelling time; 2 line Kalman averaging). Postablation conditions of experimental larvae were documented on the Leica TCS SP5 II in confocal mode (Leica 40× objective HCX PL APO CS) (148 × 148 × 35 μm for overview images and 46 × 46 × 17 μm for zoomed images; 200 Hz with 2 line averaging).

**Stimulation of Larvae.** In each assay, six 5-dpf zebrafish larvae were transferred to a hexagonal assembly of six Petri dishes (diameter 35 mm), each with 2 mL E3 medium, arranged around a vibrational speaker (PocketBoom; Mobile Fun Limited). A pulse generator (TGP110 10 MHz; AIM-TTI) delivered a single rectangular pulse (duration 100 μs, amplitude 800 mV) to the speaker. Escape responses of the larvae were recorded from below using a digital high-speed camera (3,000 frames per s [fps]; triggered to record 10 ms prior to and 100 ms after the stimulus; FASTCAM APX RS; Photron). Larvae were stimulated with a single stimulus 12 times every 10 min. They were then uni- or bilaterally ablated as described above. Control larvae were also embedded, but no M cells were ablated. Subsequently, larvae were freed and transferred to the experimental dishes to obtain responses to another set of 28 stimuli. On the second (6 dpf) and third (7 dpf) days, the larvae received a stimulus 30 times every 10 min, with a 100-min break after the first 15 stimuli. At the end of each day, larvae were transferred to fresh E3 medium with dried food (NovoTom Artemia; JBL) at 28.5 °C. To check for M cell state, larvae were embedded and imaged with the two-photon microscope (as described above) at the end of the first day and prior to the stimuli on the second and third days. We examined latency, response probability, and mean angular speed (angle of bending/time of bending). Latency is defined as time from stimulus onset to the first visible movement, and bending duration is the interval between the first movement and the time at which the body was completely bent. Angle is the maximum angle of the turn at the end of stage 1 (18). All high-speed videos were quantitatively analyzed using Fiji (52).

**Retrograde Labeling and Calcium Imaging of the Complete M Series.** *Casper* larvae were raised as described above. Larvae (5-dpf) were anesthetized in 0.04% ethyl 3-aminobenzoate methanesulfonate (MS-222) in dH<sub>2</sub>O for 5 to 10 min. Larvae were then embedded in a small Petri dish lying on their side in 1.5% low-melting-point agarose. Oregon green 488 BAPTA-1 dextran, potassium salt (10,000 MW, anionic; Invitrogen) was dissolved in 25 μL Hepes solution (10 mM Hepes, 10 mM glucose, 134 mM NaCl, 2.9 mM KCl, 2.1 mM CaCl<sub>2</sub>, 1.2 mM MgCl<sub>2</sub>, pH 7.8). Using a micromanipulator (MM-30; Märzhäuser), OGB-Hepes solution was pressure-injected (PDES-01 AM; npi Electronic) via a glass microcapillary (GB150F-8P; Science Products) into the spinal cord between the 15th and 18th somites (21, 53). Injected larvae were freed, transferred to E3 medium at 28.5 °C, and fed (dried food; NovoTom Artemia; JBL). The next day, larvae were embedded again to control for fluorescence in the M series under the two-photon microscope. Positive identified larvae (6-dpf) were then fixed again in a Petri dish (diameter 55 mm) with their dorsal side up. Stimulation then was as described. Ca<sup>2+</sup> responses in the M cells and their homologs were derived from images (296 × 87 μm) taken every 385 ms for

a total of ~19 s (per trial, 50 images were acquired with LAS AF; version 2.6.0.7266; Leica Microsystems).

**Predator–Prey Experiments.** Both M cells of 4-dpf *Ca-Tol-056* larvae were ablated as described above. On the next day, the larvae were embedded again to confirm complete absence of the soma and of the AIS—in which case the larvae were selected for predator–prey experiments on the next day. As procedural controls (sham ablations), we ablated two neurons of the cerebellum (located dorsostral to the M cells), using the exact same procedure as described above (including the same laser energy) and also with a subsequent control mimic on the following day. For predator–prey experiments, each damselfly nymph was transferred individually into a plastic tank (21.5 × 11.5 × 13 cm with 600 mL water, 24 °C) on the eighth day of the preparation phase (see above). To each damselfly nymph, we added four zebrafish larvae with successfully ablated M cells. Additionally, four nonablated zebrafish larvae of the *casper* strain were added to each nymph. Hence, survival of the ablated and nonablated larvae could directly be compared. All zebrafish were acclimated to 24 °C before facing their predator. In additional controls, each nymph faced eight nonablated *casper*, eight nonablated *Ca-Tol-056* larvae, or four sham-ablated larvae together with four nonablated *casper* larvae. We counted surviving larvae every hour. All predator–prey experiments were terminated after 7 h. All vanished larvae had been captured and eaten by the nymphs. The surviving larvae were anesthetized in 0.04% MS-222 and counted using a fluorescence stereo microscope (SMZ18; Nikon) by which the *Ca-Tol-056* larvae could be easily detected by the GFP fluorescence of their eyes.

**Escapes of Unilaterally M Cell-Ablated Adult Zebrafish.** M cells in embedded zebrafish larvae (5-dpf) were unilaterally ablated as described above and larvae were subsequently allowed to swim freely. Until 48 h after ablation, the larvae were embedded again to check the state of M cell axon degeneration under the two-photon microscope. Larvae with one AIS clearly absent were selected and raised in tanks at 28.5 °C together with their nonablated siblings. At least 5 mo later, escape responses of one individual at a time were examined in small tanks (~26 × 15 × 13 cm). The experimenter had no information on which fish had been ablated, on which side an M cell was missing, or if the experimental fish was an unablated sibling. After the experiments it was controlled for each fish if an M cell was missing and whether starts toward the left or toward the right were ipsi- or contralateral to an absent M cell. A total of 13 adult fish were analyzed. Acoustic stimuli were delivered by an active loudspeaker (box Achat 112MA; Thomann) placed about 1 m below the tank. The speaker was driven by a rectangular pulse (duration 1 ms, amplitude 3 V). Sound pressure level, measured with a hydrophone (hydrophone 8106, amplifier 2610; Brüel and Kjaer) in the tank, was 135 dB re 1 μPa, the spectral peak was at 128 Hz, and –20 dB points were at 67 and 1,100 Hz. Each animal received between 20 and 40 stimuli per d with intervals of at least 5 min between subsequent stimuli. Every fish received at least 100 stimuli. Escapes were recorded with a Phantom version 9.1 camera (Vision Research) at 1,000 fps with a resolution of 1,632 × 1,200 pixels. The analysis of the escapes was done using Fiji (52). The coordinates of the tip of the fish's mouth, the basis of the tail fin, and its center of mass were taken in three frames: 1) when the fish initiated its escape, 2) when the body was maximally bent, and 3) when the body was first straight again. A maximum of 50 videos (out of 100 to 300 videos) per fish was selected to yield between 5 and 25 videos for each of the two bending directions (“ipsi” or “contra”; see Fig. 1A). Before being analyzed by one person, these videos had been randomized by an independent second person. In this way, a total number of 515 escapes were analyzed. Individual fish contributed a minimum of 30 and a maximum of 43 escapes.

**Confirmation of Where M Axons Were Missing.** Subsequent to the behavioral experiments with the adult zebrafish, fish were killed (MS-222, 0.3 mg/mL) and then transferred to 4% PFA for at least 48 h. A piece of trunk below the dorsal fin was cut out and then sliced transversally (20 μm) in a cryostat (CM1950; Leica Biosystems). Slices were stained with FluoroMyelin (Fisher Scientific), mounted with Mowiol (2.5% DABCO; Carl Roth) on lysine-coated slides, and analyzed (Zeiss AxioScope.A1 with AxioCam ICm1) for green (GFP) and red (FluoroMyelin) fluorescence.

**Statistical Analysis.** Statistical analyses were run on Prism 5.01 (GraphPad Software). Normality was checked and either *t* tests or one-way ANOVAs (with Bonferroni-corrected *t* tests as posttests) were run or Mann–Whitney *U* tests or Kruskal–Wallis tests. Boxplots show the interquartile range of 25 to

75% with whiskers from minimum to maximum. The log-rank test was used to analyze the predator-prey experiments.

**Data Availability.** The published article contains all datasets generated during this study. Requests for further information and resources should be directed to the corresponding author.

**ACKNOWLEDGMENTS.** We thank our reviewers for many helpful remarks, for drawing our attention to the work on starburst amacrine cells, and for suggesting how soma ablations could reduce current shunted away from the AIS. We also thank Thomas Toesko, Pamela Anger, and Barbara Bekwinknoll for excellent help. The project was funded by a Koselleck award of the Deutsche Forschungsgemeinschaft (Schu1470/8).

1. K. T. Sillar, L. D. Picton, W. J. Heitler, *The Neuroethology of Predation and Escape* (Wiley, 2016).
2. S. Namiki, M. H. Dickinson, A. M. Wong, W. Korff, G. M. Card, The functional organization of descending sensory-motor pathways in *Drosophila*. *eLife* **7**, e34272 (2018).
3. D. H. Edwards, W. J. Heitler, F. B. Krasne, Fifty years of a command neuron: The neurobiology of escape behavior in the crayfish. *Trends Neurosci.* **22**, 153–161 (1999).
4. K. Lingenhöhl, E. Friauf, Giant neurons in the rat reticular formation: A sensorimotor interface in the elementary acoustic startle circuit? *J. Neurosci.* **14**, 1176–1194 (1994).
5. R. C. Eaton, *Neural Mechanisms of Startle Behavior* (Plenum, 1984).
6. H. G. Krapp, R. Hengstenberg, Estimation of self-motion by optic flow processing in single visual interneurons. *Nature* **384**, 463–466 (1996).
7. M. Papadopolou, S. Cassenaer, T. Nowotny, G. Laurent, Normalization for sparse encoding of odors by a wide-field interneuron. *Science* **332**, 721–725 (2011).
8. S. J. Zottoli, D. S. Faber, The Mauthner cell: What has it taught us? *Neuroscientist* **6**, 26–38 (2000).
9. H. Korn, D. S. Faber, The Mauthner cell half a century later: A neurobiological model for decision-making? *Neuron* **47**, 13–28 (2005).
10. R. C. Eaton, W. A. Lavender, C. M. Wieland, Alternative neural pathways initiate fast-start responses following lesions of the Mauthner neuron in goldfish. *J. Comp. Physiol.* **145**, 485–496 (1982).
11. R. DiDomenico, J. Nissarov, R. C. Eaton, Lateralization and adaptation of a continuously variable behavior following lesions of a reticulospinal command neuron. *Brain Res.* **473**, 15–28 (1988).
12. R. C. Eaton, R. DiDomenico, J. Nissarov, Role of the Mauthner cell in sensorimotor integration by the brain stem escape network. *Brain Behav. Evol.* **37**, 272–285 (1991).
13. R. C. Eaton, J. C. Hofve, J. R. Fetcho, Beating the competition: The reliability hypothesis for Mauthner axon size. *Brain Behav. Evol.* **45**, 183–194 (1995).
14. K. S. Liu, J. R. Fetcho, Laser ablations reveal functional relationships of segmental hindbrain neurons in zebrafish. *Neuron* **23**, 325–335 (1999).
15. S. J. Zottoli, B. C. Newman, H. I. Rieff, D. C. Winters, Decrease in occurrence of fast startle responses after selective Mauthner cell ablation in goldfish (*Carassius auratus*). *J. Comp. Physiol. A Neuroethol. Sens. Neural Behav. Physiol.* **184**, 207–218 (1999).
16. E. Gahtan, H. Baier, Of lasers, mutants, and see-through brains: Functional neuroanatomy in zebrafish. *J. Neurobiol.* **59**, 147–161 (2004).
17. A. M. Lacoste et al., A convergent and essential interneuron pathway for Mauthner-cell-mediated escapes. *Curr. Biol.* **25**, 1526–1534 (2015).
18. H. A. Burgess, M. Granato, Sensorimotor gating in larval zebrafish. *J. Neurosci.* **27**, 4984–4994 (2007).
19. C. B. Kimmel, R. C. Eaton, S. L. Powell, Decreased fast-start performance of zebrafish larvae lacking Mauthner neurons. *J. Comp. Physiol.* **140**, 343–350 (1980).
20. T. Kohashi, Y. Oda, Initiation of Mauthner- or non-Mauthner-mediated fast escape evoked by different modes of sensory input. *J. Neurosci.* **28**, 10641–10653 (2008).
21. D. M. O'Malley, Y. H. Kao, J. R. Fetcho, Imaging the functional organization of zebrafish hindbrain segments during escape behaviors. *Neuron* **17**, 1145–1155 (1996).
22. H. Nakayama, Y. Oda, Common sensory inputs and differential excitability of segmentally homologous reticulospinal neurons in the hindbrain. *J. Neurosci.* **24**, 3199–3209 (2004).
23. A. Nair, C. Nguyen, M. J. McHenry, A faster escape does not enhance survival in zebrafish larvae. *Proc. Biol. Sci.* **284**, 20170359 (2017).
24. P. W. Webb, Effect of body form and response threshold on the vulnerability of four species of teleost prey attacked by largemouth bass (*Micropterus salmoides*). *Can. J. Fish. Aquat. Sci.* **43**, 763–771 (1986).
25. R. DiDomenico, R. C. Eaton, Seven principles for command and the neural causation of behavior. *Brain Behav. Evol.* **31**, 125–140 (1988).
26. H. C. Howland, Optimal strategies for predator avoidance: The relative importance of speed and manoeuvrability. *J. Theor. Biol.* **47**, 333–350 (1974).
27. D. Weihs, P. W. Webb, Optimal avoidance and evasion tactics in predator-prey interactions. *J. Theor. Biol.* **106**, 189–206 (1984).
28. J. A. Walker, C. K. Ghalambor, O. L. Griset, D. McKenney, D. Reznick, Do faster starts increase the probability of evading predators? *Funct. Ecol.* **19**, 808–815 (2005).
29. C. B. Kimmel, S. K. Sessions, R. J. Kimmel, Radiosensitivity and time of origin of Mauthner neuron in the zebra fish. *Dev. Biol.* **62**, 526–529 (1978).
30. L. Conforti, J. Gilley, M. P. Coleman, Wallerian degeneration: An emerging axon death pathway linking injury and disease. *Nat. Rev. Neurosci.* **15**, 394–409 (2014).
31. M. E. Vargas, B. A. Barres, Why is Wallerian degeneration in the CNS so slow? *Annu. Rev. Neurosci.* **30**, 153–179 (2007).
32. M. Broom, G. D. Ruxton, You can run—or you can hide: Optimal strategies for cryptic prey against pursuit predators. *Behav. Ecol.* **16**, 534–540 (2005).
33. G. De Franceschi, T. Vivattanasarn, A. B. Saleem, S. G. Solomon, Vision guides selection of freeze or flight defense strategies in mice. *Curr. Biol.* **26**, 2150–2154 (2016).
34. D. Terburg et al., The basolateral amygdala is essential for rapid escape: A human and rodent study. *Cell* **175**, 723–735.e16 (2018).
35. R. E. Engeszer, L. B. Patterson, A. A. Rao, D. M. Parichy, Zebrafish in the wild: A review of natural history and new notes from the field. *Zebrafish* **4**, 21–40 (2007).
36. R. Spence, G. Gerlach, C. Lawrence, C. Smith, The behaviour and ecology of the zebrafish, *Danio rerio*. *Biol. Rev. Camb. Philos. Soc.* **83**, 13–34 (2008).
37. R. M. White et al., Transparent adult zebrafish as a tool for in vivo transplantation analysis. *Cell Stem Cell* **2**, 183–189 (2008).
38. S. Nagayoshi et al., Insertional mutagenesis by the Tol2 transposon-mediated enhancer trap approach generated mutations in two developmental genes: tcf7 and synembryo-like. *Development* **135**, 159–169 (2008).
39. S. He, R. H. Masland, Retinal direction selectivity after targeted laser ablation of starburst amacrine cells. *Nature* **389**, 378–382 (1997).
40. K. Yoshida et al., A key role of starburst amacrine cells in originating retinal directional selectivity and optokinetic eye movement. *Neuron* **30**, 771–780 (2001).
41. J. W. Scott, S. J. Zottoli, N. P. Beatty, H. Korn, Origin and function of spiral fibers projecting to the goldfish Mauthner cell. *J. Comp. Neurol.* **339**, 76–90 (1994).
42. C. Satou et al., Functional role of a specialized class of spinal commissural inhibitory neurons during fast escapes in zebrafish. *J. Neurosci.* **29**, 6780–6793 (2009).
43. M. E. Hale, H. R. Katz, M. Y. Peek, R. T. Fremont, Neural circuits that drive startle behavior, with a focus on the Mauthner cells and spiral fiber neurons of fishes. *J. Neurogenet.* **30**, 89–100 (2016).
44. K. C. Marsden et al., A Cyfip2-dependent excitatory interneuron pathway establishes the innate startle threshold. *Cell Rep.* **23**, 878–887 (2018).
45. Y. Frégnac, Big data and the industrialization of neuroscience: A safe roadmap for understanding the brain? *Science* **358**, 470–477 (2017).
46. S. W. Oh et al., A mesoscale connectome of the mouse brain. *Nature* **508**, 207–214 (2014).
47. S. J. Zottoli, L. E. Marek, M. A. Agostini, S. L. Strittmatter, Morphological and physiological survival of goldfish Mauthner axons isolated from their somata by spinal cord crush. *J. Comp. Neurol.* **255**, 272–282 (1987).
48. J. A. Blundon, R. A. Sheller, J. W. Moehlenbruck, G. D. Bittner, Effect of temperature on long-term survival of anucleate giant axons in crayfish and goldfish. *J. Comp. Neurol.* **297**, 377–391 (1990).
49. G. D. Bittner, Long-term survival of anucleate axons and its implications for nerve regeneration. *Trends Neurosci.* **14**, 188–193 (1991).
50. C. G. Gross, Genealogy of the “grandmother cell.” *Neuroscientist* **8**, 512–518 (2002).
51. R. Q. Quiroga, L. Reddy, G. Kreiman, C. Koch, I. Fried, Invariant visual representation by single neurons in the human brain. *Nature* **435**, 1102–1107 (2005).
52. J. Schindelin et al., Fiji: An open-source platform for biological-image analysis. *Nat. Methods* **9**, 676–682 (2012).
53. M. Takahashi, M. Narushima, Y. Oda, In vivo imaging of functional inhibitory networks on the Mauthner cell of larval zebrafish. *J. Neurosci.* **22**, 3929–3938 (2002).